

Evolutionary and Pulsational Properties of Ultra-massive White Dwarfs. The Role of Oxygen-Neon Phase Separation.

F. C. De Gerónimo,^{1,2} M. E. Camisassa^{1,2}, A. H. Córscico^{1,2}, L. G. Althaus,^{1,2}

¹Facultad de Ciencias Astronómicas y Geofísicas, Universidad Nacional de La Plata, Paseo del Bosque s/n, (1900) La Plata, Argentina; fdegeronimo@fcaglp.unlp.edu.ar

²Instituto de Astrofísica de La Plata, CONICET-UNLP

Abstract

Ultra-massive hydrogen-rich white dwarf stars are expected to harbour oxygen/neon cores resulting from semidegenerate carbon burning when the progenitor star evolves through the super asymptotic giant branch (S-AGB) phase. These stars are expected to be crystallized by the time they reach the ZZ Ceti domain. We show that crystallization leads to a phase separation of oxygen and neon in the core of ultra-massive white dwarfs, which impacts markedly the pulsational properties, thus offering a unique opportunity to infer and test the process of crystallization and phase separation in white dwarf stars.

1 Methodology & Input Physics

We computed the evolution (Camisassa et al., 2018) and pulsation properties (De Gerónimo et al., 2018) of ultra-massive DA (hydrogen-rich) WD sequences with stellar masses $M_* = 1.10, 1.16, 1.22, \text{ and } 1.29 M_\odot$ (Fig. 1) resulting from the complete evolution of the progenitor stars through the S-AGB phase (Siess, 2010). Prior evolution provides us with realistic core chemical profiles, envelope stratification, and helium mass. In Table 1 we show the H and He mass of our models, together with the effective temperature and surface gravity at the onset of crystallization, and the fraction of crystallized mass at the blue and red edges of the ZZ Ceti instability strip. The cores are composed mostly of ^{16}O and ^{20}Ne and smaller amounts of ^{12}C , ^{23}Na and ^{24}Mg . The H content is set to $M_{\text{H}} \sim 10^{-6} M_*$.

Nonradial g (gravity)-mode pulsations of our complete set of ultra-massive ONe-core DA WD models were computed using the adiabatic version of the LP-PUL pulsation code. The pulsation code is based on the general Newton-Raphson technique that solves the full fourth order set of equations and boundary conditions governing linear, spheroidal, adiabatic, non-

radial stellar pulsations following the dimensionless formulation of Dziembowski (1971). To account for the effects of crystallization on the pulsation spectrum of g modes, we adopted the “hard sphere” boundary conditions, which assume that the amplitude of the eigenfunctions of g modes is drastically reduced below the solid/liquid interface due to the non-shear modulus of the solid, as compared with the amplitude in the fluid region (see Montgomery & Winget, 1999).

The DA WD evolutionary models developed in this work were computed with the amply used LPCODE evolutionary code. This code considers all the physical ingredients involved in white dwarf modeling, including element diffusion. In this work we included, *for the first time*, both energy release and chemical abundance changes caused by the process of phase separation during crystallization. We considered the phase diagram of Medin & Cumming (2010), suitable for the dense plasmas of oxygen/neon mixtures appropriate for ultra-massive white dwarfs. For the CO-core sequences, crystallization was considered following the phase diagram of Horowitz et al. (2010). Phase diagrams provide us with the temperature at which crystallization occurs and the resulting abundances of the solid phase. To our knowledge, this is the *first* evolutionary and pulsational analysis of ultra-massive DA WD models that includes phase separation processes in ONe cores.

2 Results

In Fig. 1 we show the $\log(g) - T_{\text{eff}}$ plane of our WD sequences, computed for this work. In addition, we plot the isochrones of 0.1, 0.5, 1, 2 and 5 Gyr (blue lines) together with the sample of currently known ultra-massive non-variable DAs (black crosses) and ultra-massive variable DAs, known as ZZ Ceti (red squares)

We found strong differences in the pulsation spectra of our WD models for the different cases analyzed. In particular, we found notable differences in the period spacings for the case in which the changes in the core

M_*/M_\odot	M_{He}/M_* ($\times 10^{-5}$)	T_{eff}^c (K)	$\log g^c$ (cgs)	M_c/M_* ($T_{\text{eff}} = 12\,500$ K)	M_c/M_* ($T_{\text{eff}} = 10\,500$ K)
1.098	29.6	19881	8.83	0.81	0.92
1.159	15.7	23291	8.95	0.90	0.96
1.226	6.38	28425	9.12	0.96	0.98
1.292	1.66	37309	9.33	0.994	0.998

Table 1: H and He mass content of our ONe-core ultra-massive DA WD models, together with the effective temperature and surface gravity at the onset of crystallization, and the fraction of crystallized mass at the blue and red edges of the ZZ Ceti instability strip.

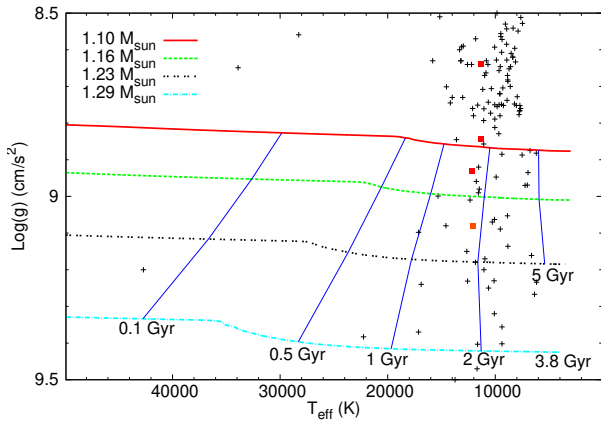


Figure 1: Hydrogen-rich WD model sequences in the $\log(g) - T_{\text{eff}}$ plane. Blue solid lines display isochrones of 0.1, 0.5, 1, 2, and 5 Gyr. Black crosses indicate the location of a sample of ultra-massive DA white dwarfs. Red squares display ultra-massive ZZ Ceti stars.

chemical profiles due to phase separation are taken into account (Fig. 2), as compared with the case in which they are ignored. This is borne out in the upper central and right panels of Fig. 3. *These differences could be exploited as an asteroseismological tool in real ZZ Ceti stars to elucidate if phase separation during crystallization occurs in the deep interior of WD stars.*

We also compared the pulsation properties of WD models characterized by the same stellar mass ($1.10M_\odot$) but in one case having a core made of ^{16}O and ^{20}Ne and in another case a core composed by ^{12}C and ^{16}O . We did not find sizable differences in either the mean period spacing or the period-spacing distribution (Fig. 4) at the ZZ Ceti stage. So, we conclude that these pulsation quantities do not allow for differentiation of the chemical composition of the cores of ultra-massive ZZ Ceti stars.

3 Conclusions

We show that ultra-massive pulsating DA white dwarfs are, in principle, powerful tools to investigate the existence of phase-separation processes occurring in their interiors, thus representing an independent avenue to

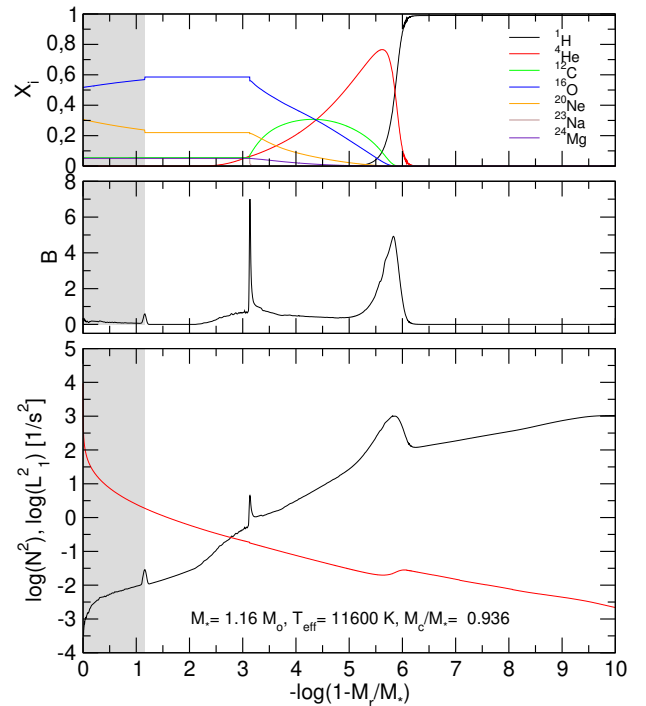


Figure 2: Chemical profiles (upper panel), the Ledoux term B (middle panel), and the logarithm of the squared Brunt-Väisälä and Lamb frequencies (lower panel), corresponding to a ONe-core WD model with $M_* = 1.16M_\odot$, $T_{\text{eff}} \sim 11\,600$ K. The gray area marks the domain of crystallization. M_c/M_* is the crystallized mass fraction of the model.

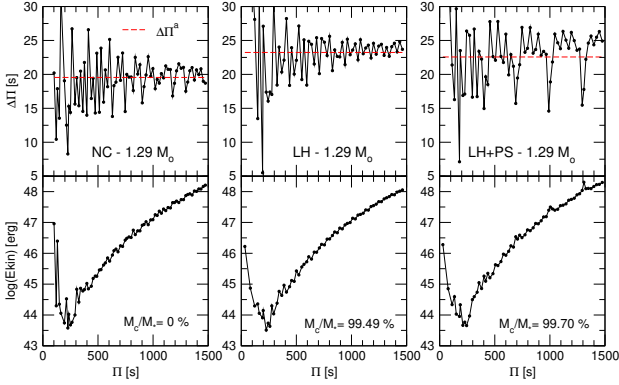


Figure 3: Forward period spacing (upper panels) and the logarithm of the oscillation kinetic energy (lower panels) in terms of the periods of $\ell = 1$ pulsation modes for a $1.29M_{\odot}$ ONE-core WD model at $T_{\text{eff}} \sim 11\,600$ K. In the left panels crystallization has not been taken into account (NC case), while the central panels show the situation in which crystallization has been considered but phase separation has been neglected (LH case). The right panels show the case in which both crystallization and phase separation have been taken into account (LH+PS case). In the upper panels, horizontal red dashed lines correspond to the asymptotic period spacing.

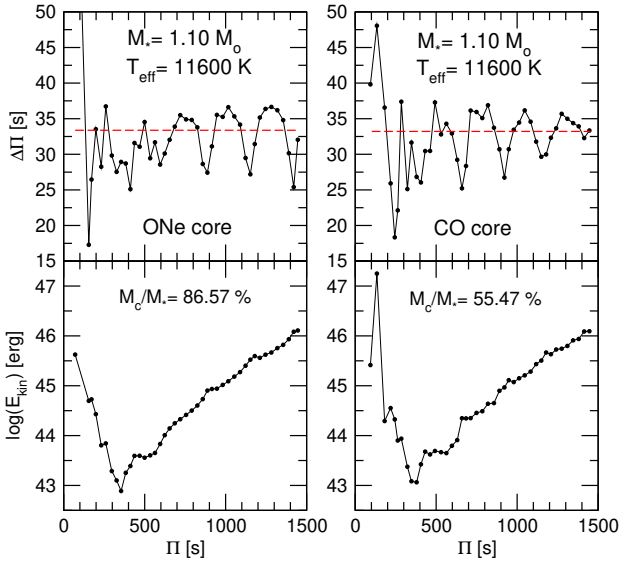


Figure 4: The forward period spacing (upper panels) and the logarithm of the oscillation kinetic energy (lower panels) in terms of the periods of $\ell = 1$ pulsation modes for a $1.10M_{\odot}$ WD model at $T_{\text{eff}} \sim 11\,600$ K with a ONE core (left panel) and a CO core (right panel). In both models, latent heat release and chemical redistribution due to phase separation have been taken into account during crystallization (LH+PS case). The percentage of the crystallized mass is indicated for both models.

confirm the results derived from studies of the WD luminosity function of stellar clusters (Winget et al., 2009; García-Berro et al., 2010) about the occurrence of crystallization in WDs.

We believe that in order to infer the core composition of ultra-massive DA WDs it will be necessary to carry out detailed asteroseismic analyses using the individual periods observed in ultra-massive ZZ Ceti stars like BPM 37093 (Kanaan et al., 1992, 2005), GD 518 (Hermes et al., 2013), and SDSS J0840+5222 (Curd et al., 2017).

Evolutionary sequences can be found at: <http://evolgroup.fcaglp.unlp.edu.ar/TRACKS/DA.html>

References

- Camisassa M. E., et al., 2018, preprint, (arXiv:1807.03894)
- Curd B., Gianninas A., Bell K. J., Kilic M., Romero A. D., Allende Prieto C., Winget D. E., Winget K. I., 2017, MNRAS, 468, 239
- De Gerónimo F. C., Córscico A. H., Althaus L. G., Wachlin F. C., Camisassa M. E., 2018, preprint, (arXiv:1807.03810)
- Dziembowski W. A., 1971, actaa, 21, 289
- García-Berro E., et al., 2010, Nature, 465, 194
- Hermes J. J., Kepler S. O., Castanheira B. G., Gianninas A., Winget D. E., Montgomery M. H., Brown W. R., Harrold S. T., 2013, ApJ, 771, L2
- Horowitz C. J., Schneider A. S., Berry D. K., 2010, Physical Review Letters, 104, 231101
- Kanaan A., Kepler S. O., Giovannini O., Diaz M., 1992, ApJ, 390, L89
- Kanaan A., et al., 2005, A&A, 432, 219
- Medin Z., Cumming A., 2010, Phys. Rev. E, 81, 036107
- Montgomery M. H., Winget D. E., 1999, ApJ, 526, 976
- Siess L., 2010, A&A, 512, A10
- Winget D. E., Kepler S. O., Campos F., Montgomery M. H., Girardi L., Bergeron P., Williams K., 2009, ApJ, 693, L6